Cell

A Physical and Regulatory Map of Host-Influenza Interactions Reveals Pathways in H1N1 Infection

Sagi D. Shapira,[1,2,3,8] Irit Gat-Viks,[1,8] Bennett O.V. Shum,[1] Amelie Dricot,[4,6] Marciela M. de Grace,[1,2,5] Liguo Wu,[1,2,3] Piyush B. Gupta,[1] Tong Hao,[4,6] Serena J. Silver,[1] David E. Root,[1] David E. Hill,[4,6] Aviv Regev,[1,7,9,*] and Nir Hacohen[1,2,3,9,*]
[1]Broad Institute of MIT and Harvard, 7 Cambridge Center, Cambridge, MA 02142, USA
[2]Center for Immunology and Inflammatory Diseases, Massachusetts General Hospital, 149 13th Street, Charlestown, MA 02129 USA
[3]Department of Medicine
[4]Department of Genetics
[5]Program in Virology
Harvard Medical School, Boston, MA 02115, USA
[6]Center for Cancer Systems Biology and Department of Cancer Biology, Dana-Farber Cancer Institute, 44 Binney Street, Boston, MA 02115, USA
[7]Howard Hughes Medical Institute, Department of Biology, Massachusetts Institute of Technology, Cambridge, MA 02142, USA
[8]These authors contributed equally to this work
[9]These authors contributed equally to this work
*Correspondence: aregev@broad.mit.edu (A.R.), nhacohen@partners.org (N.H.)
DOI 10.1016/j.cell.2009.12.018

SUMMARY

During the course of a viral infection, viral proteins interact with an array of host proteins and pathways. Here, we present a systematic strategy to elucidate the dynamic interactions between H1N1 influenza and its human host. A combination of yeast two-hybrid analysis and genome-wide expression profiling implicated hundreds of human factors in mediating viral-host interactions. These factors were then examined functionally through depletion analyses in primary lung cells. The resulting data point to potential roles for some unanticipated host and viral proteins in viral infection and the host response, including a network of RNA-binding proteins, components of WNT signaling, and viral polymerase subunits. This multilayered approach provides a comprehensive and unbiased physical and regulatory model of influenza-host interactions and demonstrates a general strategy for uncovering complex host-pathogen relationships.

INTRODUCTION

Mammalian cells have developed complex systems to detect and eliminate viral pathogens, while viruses have evolved mechanisms to co-opt host processes and suppress host defenses. For example, influenza A is a segmented, single-stranded, negative-sense RNA virus that has adapted to infect multiple species. Upon infection by influenza, host cells detect viral RNA through pathogen sensors, such as RIG-I, and induce type I interferons (IFNs) and an antiviral program that is common to many RNA viruses (Figure 1A) (Takeuchi and Akira, 2009). At the same time, the ten major (and one minor) gene products of influenza virus mediate the viral life cycle and modulate cellular processes. Most notably, the NS1 protein subverts host defenses through several mechanisms, including suppression of RIG-I/TRIM25-mediated sensing of viral RNA (Gack et al., 2009; Pichlmair et al., 2006), PKR antiviral activity (Li et al., 2006), and cellular mRNA processing (Krug et al., 2003). Immune regulatory functions for the other influenza proteins have yet to be defined, as their assigned roles have been limited to viral entry into cells, viral RNA trafficking, replication, and transcription, as well as assembly of mature virions. Similarly, the function of the vast majority of host factors remains unexplored. Previous studies on viral and host factors have focused on specific interactions but have not produced global models of the viral-host relationship, with few exceptions (Brass et al., 2008; Bushman et al., 2009; König et al., 2008; Krishnan et al., 2008; Li et al., 2009).

Here, we use an integrative functional genomics strategy (Figures 1B–1D) to generate a draft model of influenza-host interactions for the H1N1 strain A/PR/8/34 ("PR8"). Our experimental and computational approach uncovers host networks contacted by viral proteins, cellular transcriptional responses to infection, and functional roles for candidate factors in influenza-infected primary lung epithelial cells. We integrate these datasets to generate a physical, regulatory, and functional map that implicates hundreds of host factors in the influenza-human relationship.

RESULTS

Identification of a Human Protein Network that Physically Interacts with Ten Viral Proteins

To identify host factors that may participate in the pathogenesis of influenza infection, we first sought to identify those factors that

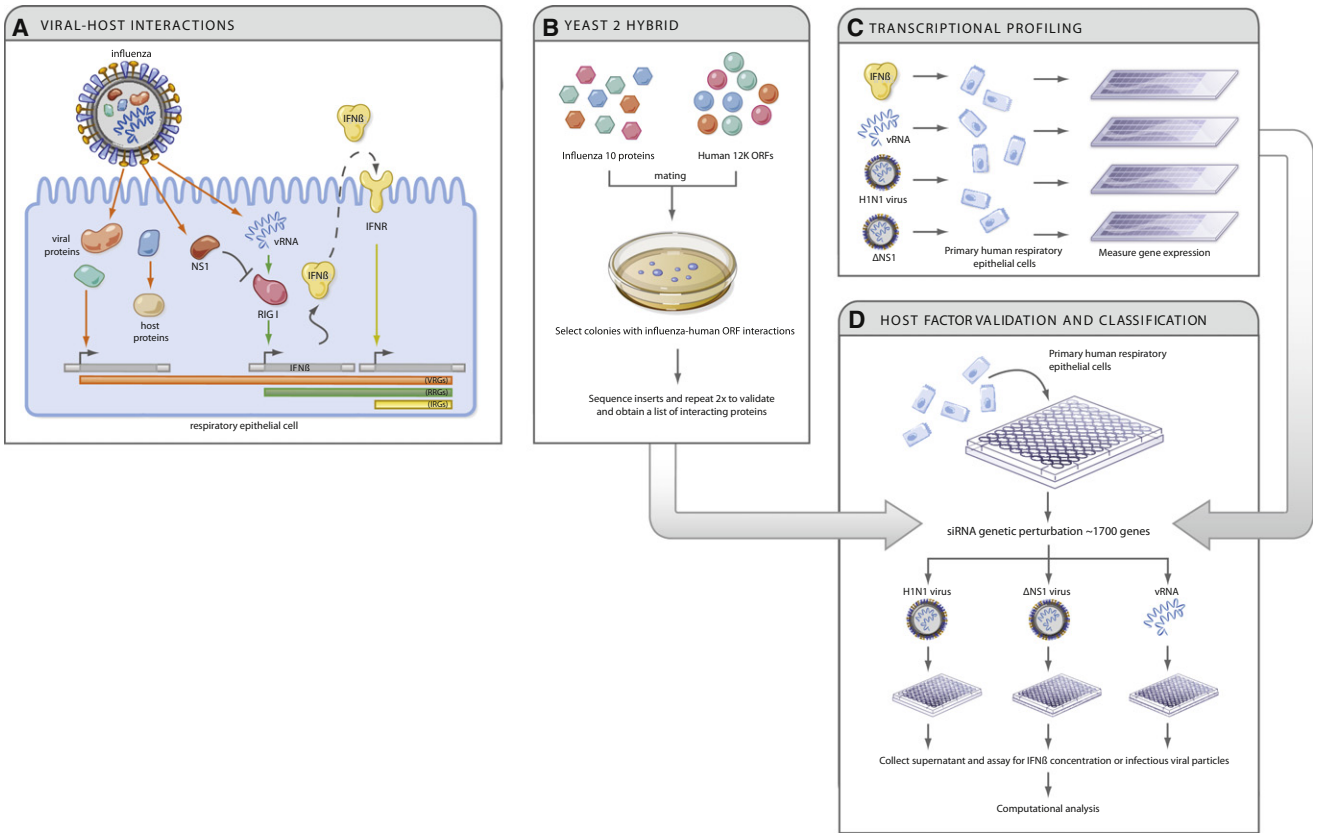

Figure 1. Integrative Strategy to Generate a Physical, Regulatory, and Functional Map of Influenza-Host Interactions

(A) When influenza infects host cells, viral components, including viral RNA (vRNA) and viral proteins, interact with host proteins to induce changes in host gene expression and cellular functions. The RIG-I sensor detects virus-derived RNA and regulates host gene expression, including IFNβ, which in turn activates an antiviral program through the interferon receptor (IFNR). We distinguish viral-regulated genes (VRGs, orange), affected by infection, RNA-regulated genes (RRGs, green), affected directly by vRNA, and interferon-regulated genes (IRGs, yellow), affected directly by interferon treatment. NS1 is known to inhibit the RIG-I response.

(B–D) A genomic strategy to deconstruct influenza-host interactions. Host proteins that physically interact with each of the ten viral proteins are identified with a systematic yeast two-hybrid approach (B), and arrays are used to define the transcriptional responses of primary human bronchial epithelial cells (HBECs) to components of the virus and to virus infection (C). The physical and transcriptional maps were used to computationally predict human factors and pathways that affect the viral life cycle or host response. We tested these predictions by perturbing each gene and measuring the effect on IFN production and viral replication in primary HBECs (D).

are directly manipulated through physical associations with viral proteins. We used a yeast two-hybrid (Y2H) approach to systematically identify direct binary contacts among the ten major viral proteins of the PR8 strain, as well as between each viral protein and each of ~12,000 human proteins available in the Human ORFeome v3.1 collection (Lamesch et al., 2007). We discovered 31 intraviral interactions (out of 55 possible interactions, including homodimers) among the ten viral proteins (Figure 2A, Table S1 part A available online), and 135 pairwise interactions between the ten viral proteins and 87 human proteins ("H_1" genes, Figure 2B, Table S1 part B), 73 of which are expressed in primary human bronchial epithelial cells (HBECs). These included the previously reported association between NS1 and STAU1, interactions between NS1 and PRKRA and TARBP2 (regulators of PKR-mediated transcription; for a review of NS1-host interactions, see Hale et al. [2008]), and interactions between influenza and eight proteins that are targeted by other viruses (Table S1 part B). Several known associations were not observed, either because the interacting protein was not among the 12,000 proteins in our assays (e.g., TRIM25 [Gack et al., 2009] and DDX58/RIG-I [Pichlmair et al., 2006]), or for unknown reasons (e.g., we did not detect the PKR-NS1 interaction [Li et al., 2006], yet we identified the kinase that phosphorylates PKR).

The connectivity pattern of the intraviral and viral-human network revealed three important principles. First, the influenza intra-viral network is extremely interconnected (Figure 2A, Table S2 part A), consistent with findings from other viruses (Bailer and Haas, 2009). This may be required for forming compact virions and functional viral complexes. Second, influenza proteins interact on average with a significantly greater number of human proteins than expected from the human interaction network (13.5 versus 6.5 expected, $p < 0.06$, permutation test), even when compared to other viruses (Table S2 part A), or

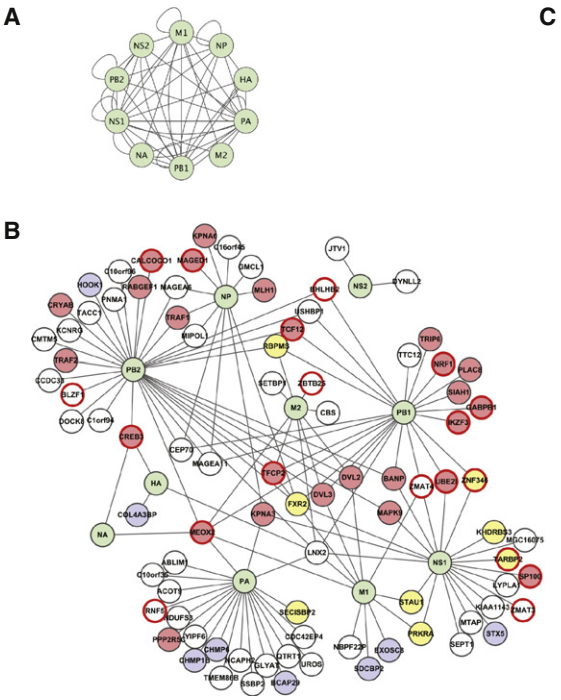

Figure 2. A Map of Viral-Human Protein Interactions Identifies a Dense Interconnected Network, Coupled to Key Cellular Signaling Pathways

(A) Viral-viral interactions. Green nodes, viral proteins; edges, direct physical interactions observed in a Y2H assay.

(B) Influenza-human interactions. One hundred and thirty-four interactions (edges) connect the ten influenza proteins (green nodes) to 87 "H1" human proteins. Yellow fill, RNA-binding proteins; blue fill, protein transport; red border, transcription factors; red fill, 30 proteins that play a role in four major signaling pathways (NFκB, apoptosis, MAPK, and WNT signaling); white fill, proteins with other functions.

(C) Thirty host interactor proteins (H_1) are shown with their membership in specific pathways (red) or direct interactions with influenza proteins (light green). H_1 proteins are either known components or have established interactions with components of these pathways (see the Experimental Procedures). Many of the 30 proteins are involved in multiple signaling pathways, and interact with polymerase subunits. Influenza A proteins: PB1, PB2, and PA (viral polymerase subunits); NP (nucleocapsid protein), involved in viral RNA transport, packaging, and polymerase functions; HA (hemagglutinin) mediates entry; NA (neuraminidase) aids in release of viral particles; M1 (matrix protein) mediates export and assembly of RNA and viral particles; M2 (matrix protein) modulates fusion through its proton channel activity; NS1 (nonstructural protein) regulates host pathways; and NS2 (nonstructural protein), involved in RNA export.

when comparing to the full 12,000 prey human network (data not shown). This may reflect the fact that a virus has to maximize the diversity of functions per protein. Third, some of the human proteins contact a greater than expected number of influenza proteins (24 human proteins interact with at least two flu proteins, $p < 10^{-5}$, permutation test, Figure 2B, Table S2 part B). These may be required for the formation of viral-host multiprotein complexes.

The H_1 proteins form interconnected hubs within the cellular protein network, suggesting that the virus targets proteins that play a central role in their respective cellular pathways. The 87 H_1 proteins connect with each other through 51 interactions and with other human proteins (first neighbors; "H_2" genes) through 2717 interactions, a higher than expected connectivity ($p < 10^{-5}$, permutation test). The higher density of interactions is observed even when excluding the most highly connected H_1 proteins, or when considering only the H_1 proteins associated with individual viral proteins (Table 1).

Furthermore, we identified a core cellular subnetwork that is enriched for H_1 proteins ($p < 0.05\text{-}10^{-4}$, hypergeometric test; Experimental Procedures, Table S3). This subnetwork contains six H_1 proteins that bind at least three other H_1 proteins (e.g., TRAF2, DVL2, and FXR2) and 37 non-H_1 proteins that fit the same criteria (e.g., p53, PKR, ILF3, and PSMF1, none of which contacts any viral protein directly). The network (Figure S1) consists of diverse proteins including RNA-binding proteins,

Table 1. Network Parameters of Influenza and Cellular Protein Interaction Networks

Network Parameters	All-H_1	All-H_1H_2	PB1-H_1	PB2-H_1	PA-H_1	NP-H_1	M1-H_1	M2-H_1	NS1-H_1	NS2-H_1	HA-H_1	NA-H_1	H. Sapiens
Nodes	87	653	23	32	21	12	11	9	20	2	3	2	11,624
Total edges	2768	17,106	1312	1640	156	686	378	384	549	50	9	11	57,206
Average Degree	34.4	30.6	60.0	55.4	8.2	57.3	37.8	48.3	32.5				9.9
Stdev Degree	42.9	43.6	50.3	49.6	7.7	36.2	40.6	48.7	47.1				19.9
Median Degree	17	15	53	47	5	59	31	32	17				4

The parameters in this table quantify the numbers of interactions between a defined set of proteins (one set in each column) with the entire human interaction network (see the Experimental Procedures). For example, there are 87 H_1 proteins (i.e., direct interactors with the 10 PR8 viral proteins) that interact with 2768 human proteins with an average of 34.4 interactions per H_1 protein (with standard deviation of 42.9). The All-H_1H_2 set includes the 87 H_1 proteins and 566 H_2 proteins that interact with them based on curated associations. X-H_1 consists of the direct human interactors of the viral protein X.

regulators of ubiquitination and sumoylation, transcription factors, mediators of apoptosis, and components of immune signaling pathways (Figures 2B, 2C, S1 and S2).

Our observations also hold in another influenza strain, the H3N2 A/Udorn/72 influenza virus ("Udorn"). Using the same Y2H approach, we detected 81 interactions between ten Udorn viral proteins and 66 human proteins. Of these, 56 human proteins also interact with PR8 ($p < 10^{-10}$, hypergeometric test; Table S1 part C and Figure S3A), including most RNA-binding proteins, regulators of transcription, protein transport, and signaling (Figure S3B). For example, out of 30 signaling proteins and 19 transcription factors that directly interact with PR8 (Figures 2B and 2C), 28 and 16 proteins (respectively) also directly bind to Udorn proteins (Figure S3B). Most (63%) of the H_1 proteins that were associated with PR8 NS1, NP, or the polymerase subunits (PB1, PB2, PA) were also found to interact with their counterparts in the Udorn strain (Figure S3C and Table S1 part B), reflecting conserved functions of viral proteins.

Viral Proteins Interact with the NF-κB, Apoptosis, and WNT Pathways Primarily through NS1 and Polymerase Subunits

To identify the key cellular pathways coupled to the virus, we considered the 87 H_1 and 566 H_2 cellular proteins from a manually curated database (IPA) and found that they are enriched for components of several signaling pathways (Table S4 part A, Figure 3D; see the Experimental Procedures). Thirty of the 87 H_1 interactors couple the virus to six major pathways, including p53-, PML- and TNFR/Fas-mediated apoptosis, NF-κB, and WNT/β-catenin (Figure 2C). The interactions with these pathways are conserved for the Udorn strain (Figure S3C), suggesting that the discovered interactions reflect a generalized strategy of influenza to manipulate the host. A role for these pathways in viral infections has been described (e.g., p53, Turpin et al. [2005]), yet their direct physical association with influenza proteins was not previously reported.

While NS1 is considered the major viral protein to modulate host signaling, we found that 26 of the 30 H_1 proteins associated with these pathways interact with viral polymerase subunits and NP, but only eight interact with NS1 (Figure 2C). In particular, H_1 and H_2 interactors of PB1, PB2, NP are highly enriched ($p < 10^{-10}$, Fisher's combined probability test) for the six key pathways, but those of PA are not (Figure 3D; this result also holds for Udorn, Figure S3C). This suggests that viral polymerase proteins may also act as direct modulators of host signaling pathways.

Expression Profiling of the Response to Viral Infection in Primary Human Lung Epithelial Cells

We next defined the major transcriptional responses in primary HBECs after either infection with influenza or treatment with relevant ligands. We used four different strategies, each highlighting distinct components of the response: (1) We infected cells with the wild-type PR8 influenza virus that can mount a complete replicative cycle. (2) We transfected cells with viral RNA (vRNA) isolated from influenza particles. This does not result in the production of viral proteins or particles and identifies the effect of RNA-sensing pathways (e.g., RIG-I.). (3) We treated cells with interferon beta (IFNβ) to distinguish the portion of the response that is mediated through type I IFNs. (4) We infected cells with a PR8 virus lacking the NS1 gene (ΔNS1). The NS1 protein normally inhibits vRNA- or IFNβ-induced pathways, and its deletion can reveal an expanded response to infection. We could not assess the role of any other viral protein but NS1, since deletion strains cannot be propagated easily (Wressnigg et al., 2009). For each of the four stimuli, we profiled the cellular transcriptional response at ten time points (0.25, 0.5, 1, 1.5, 2, 4, 6, 8, 12, and 18 hr) in duplicate experiments.

Transcription Patterns Distinguish Interferon-, RNA- and Virus-Responsive Genes

We found 12 major temporal and functional patterns of gene expression (C_1–C_{12}, Figures 3A and 3B), each associated with at least one stimulus, and covering 1056 genes that were all regulated in response to viral infection (virus-regulated genes [VRGs]). Among these, we found 666 interferon-regulated genes (IRGs) that are affected by interferon directly (325 induced, C_1–C_4, and 341 repressed, C_9–C_{10}, Figures 3A–3C). All of the IRGs are similarly affected by vRNA transfection and ΔNS1 virus but with an observed time delay, likely due to the induction of IFNβ by these stimuli. PR8 infection induces IRGs to a much lower level (with few exceptions, C_2, 57 genes), and abrogates the downregulation of 49 IRGs (C_9). This is consistent with the known role of NS1 in dampening RNA sensing and downstream interferon production (Pichlmair et al., 2006) (Figure S4).

Next, we found 721 RNA-regulated genes (RRGs) that are directly modulated by transfected vRNA (380 induced, C_1–C_5; 341 repressed, C_9–C_{10}, Figures 3A–3C). All of the RRGs are similarly affected by ΔNS1 virus infection, while 171 are regulated by PR8 infection. Thus, viral RNA present in the infecting virion and produced during modest viral replication (as with ΔNS1 virus) can induce a potent response. Induced RRGs (C_1–C_5) were enriched for antigen presentation, apoptosis, NFκB and IRF signaling ($p < 10^{-4}$–10^{-17}; hypergeometric test, Figure 3D).

Most of the induced RRGs are also induced by interferon treatment (C_1–C_4, 325 of 380), but a few IFNβ-independent RRGs (C_5) are induced only by vRNA and ΔNS1 virus. These include important antiviral genes (e.g., IFNB1, IL7R, ING3, IRF2, and PELI1) and are enriched for TLR pathway components, cytokines, chemokines, and cell cycle and apoptosis ($p < 10^{-3}$, Figure 3D). An IFNβ-independent mechanism (e.g., IRF3-dependent based on promoter sequence analysis, data not shown) is likely to mediate the transcription of these genes.

Finally, we identified virus-specific response genes (VSRGs) that are transcriptionally regulated after PR8 or ΔNS1 virus infection, but not after vRNA transfection or IFNβ treatment (C_6–C_8 and C_{11}–C_{12}). Sixty-eight VSRGs are induced only by ΔNS1 (C_6) and are enriched for regulators of apoptosis and NFκB (e.g., BCL10, TRAF6, NFKB1, and NFKBIE). NS1 may block their induction and dampen the NFκB pathway by an unknown RNA- and IFN-independent mechanism. Sixty VSRGs are induced by both PR8 and ΔNS1 (C_7) and are enriched for regulators of apoptosis, cell cycle, and transcription factors ($p < 10^{-3}$, Figure 3D). Finally, 31 VSRGs (C_8) are induced only by PR8, possibly directly by NS1 or as the result of the higher burden of a replicating virus.

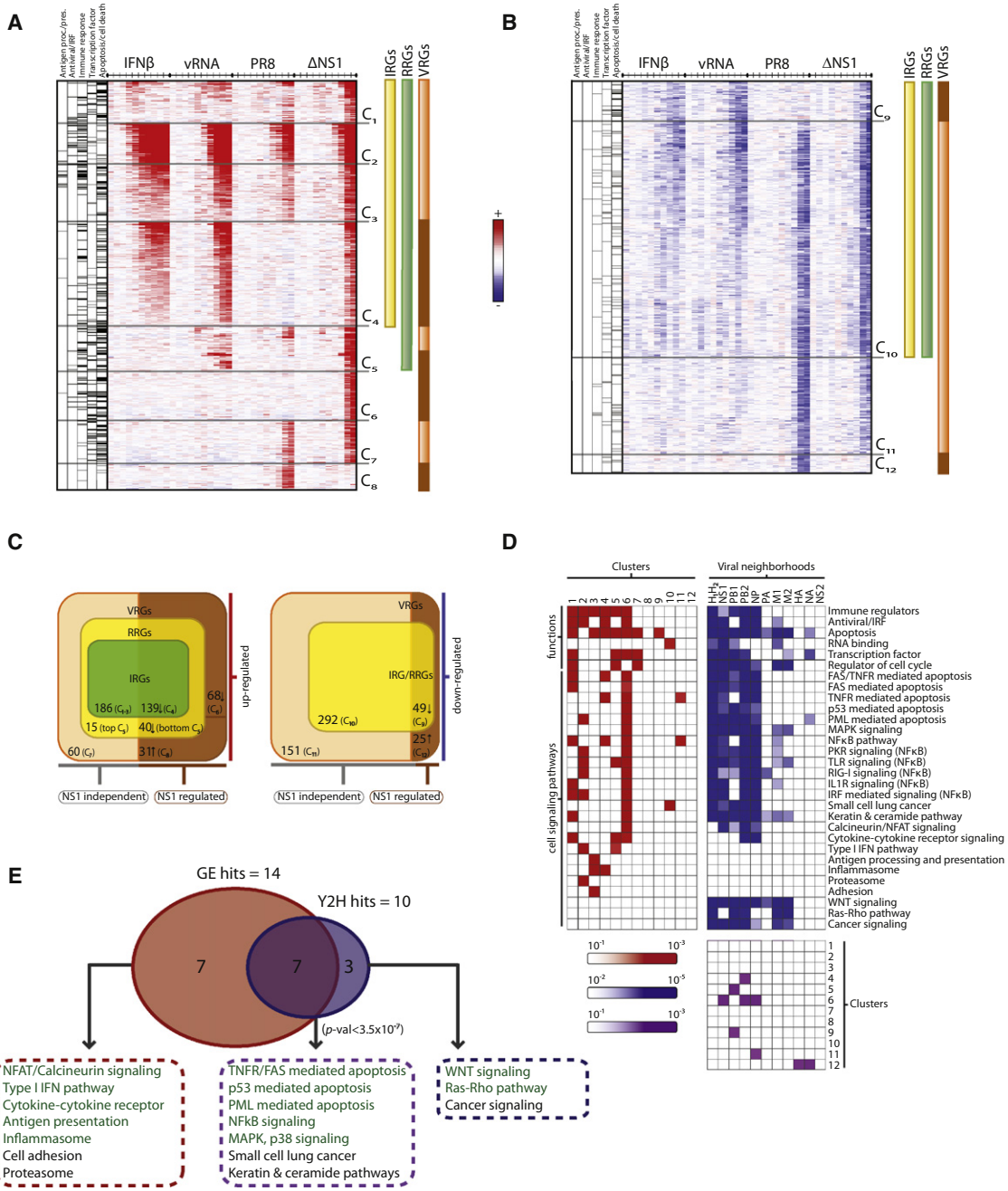

Figure 3. Distinct Transcription Patterns of Interferon-, RNA-, and Virus-Responsive Genes

(A and B) Gene expression changes in HBECs in response to IFNβ (IRGs, yellow bar), vRNA (RRGs, green bar), wild-type influenza (PR8) and mutant ΔNS1 virus (VRGs, orange bar; genes differentially regulated by NS1, brown bar) at ten time points (0.25, 0.5, 1, 1.5, 2, 4, 6, 8, 12, and 18 hr, tick marks). Genes that were upregulated (A, red) and downregulated (B, blue), relative to the expected level from mock-treated cells, were grouped into 12 clusters (C_1–C_{12}). Left columns denote gene membership in five major functional categories (black lines, category is enriched in cluster; gray lines, category is not enriched in cluster).

(C) Venn diagrams indicate number of members in each class of regulated genes and their dependence on NS1 (bottom), within the subset of upregulated (left) and downregulated (right) genes.

(D) Functional and pathway annotation of expression clusters and interaction neighborhoods. Shown are the functional categories and pathways (rows) enriched in each of the 12 expression clusters (red, left matrix) and interaction neighborhoods (H_1 and H_2) of each viral protein (blue, right matrix). The bottom matrix shows the significant overlaps (purple) between expression clusters (1–12, rows) and viral neighborhoods (columns).

(E) Enrichment analysis identifies pathways that are overrepresented in the influenza physical network (ten pathways, blue) and in transcriptional responses (14 pathways, red), with an overlap of seven pathways enriched in both (purple, $p < 3.5 \times 10^{-7}$). Pathways chosen for functional follow-up assays are colored in green.

NF-κB, MAPK, and Apoptosis Pathways Are Regulated through Both Transcriptional and Physical Interactions

Some of the host systems affected at the transcriptional level by viral infection may be linked to the virus through physical interactions. Indeed, we found that the cellular network of direct interactors (H_1) and first neighbors (H_2) is enriched for genes that are transcriptionally regulated upon viral infection (70 of 1056 VRGs, $p < 4 \times 10^{-4}$, hypergeometric test). For example, the NS1 neighborhood is enriched in C_6 ($p < 0.01$), a VSRG cluster induced only in response to infection with ΔNS1 virus (e.g., NFKB1, BCL10). Similarly, the neighborhood of the polymerase subunit PB2 and NP is also enriched in C_6 ($p < 7 \times 10^{-4}$), further supporting the potential role of the viral polymerase in modulating host pathways in concert with NS1.

While some cellular pathways are uniquely associated with either the physical network (e.g., WNT, Ras/Rho) or transcriptional responses (e.g., type I IFN and antigen presentation), many are enriched for both ($p < 3.5 \times 10^{-7}$, hypergeometric test, Figures 3D and 3E). These include p53-mediated apoptosis, PML, NFκB, MAPK, and p38 signaling. These pathways are mostly associated with rapidly and highly induced IRGs (C_2) or VSRGs that are inhibited by NS1 (C_6). Thus, the virus physically engages critical pathways while inducing transcriptional changes in their components.

Functional Interrogation of Viral Interactors and Transcriptionally Responsive Genes

The physical interactions, transcriptional responses, and associated pathways together identified 1745 candidate genes that could impact influenza infection. These included 1056 genes that were transcriptionally regulated, 259 direct interactors and their first neighbors (H_1/H_2) (67 of them are also transcriptionally regulated), and 504 further candidates predicted from our analyses (e.g., pathway members) that are expressed in HBECs.

To test the functional contribution of these genes to viral replication and type I IFN production, we measured the effect of perturbing each gene using targeted small interfering RNA (siRNA) pools in three functional assays. In the viral replication assay, we infected siRNA-transfected primary HBECs with PR8 virus and measured virus production after 48 hr using a cellular reporter system that is analogous to conventional plaque assays (Experimental Procedures). In two independent assays, we used a reporter cell line to measure levels of IFNβ in siRNA-transfected HBECs in response to ΔNS1 virus infection or vRNA transfection.

We determined the relative effect of each of the 1745 siRNA pools in each assay using a statistical scoring approach (Experimental Procedures) that identifies significant changes in phenotypes relative to the background of all tested genes. Since we selected a focused set of candidates for functional testing, this scoring approach is highly conservative. Furthermore, because cell number impacts production of IFN, we used AlamarBlue to determine cellular viability following siRNA knockdown and to effectively normalize IFN values to the number of cells in each well. We used a 2-fold threshold (Experimental Procedures) to identify genes whose perturbation significantly impacted the phenotypes evaluated in each of the three assays, distinguishing positive and negative regulators of each phenotype.

Six hundred and sixteen of the 1745 candidate genes affected at least one of the phenotypes significantly. The number of genes with two or more significant phenotypes is substantially higher than expected by chance ($p < 10^{-4}$, permutation test, Figure S5). These included all the major sources of candidate genes, including 361 transcriptionally responsive genes, 88 direct interactors (H_1) and first neighbors (curated H_2), and 174 additional members of identified pathways. This suggests that many of the transcriptional and physical target pathways play an important role in infection.

Distinct Functional Signatures for Regulators of IFN Production and Viral Replication

We divided the 616 validated genes into 20 "phenoclusters" on the basis of the combinatorial behavior of each gene across the three functional assays (Figure 4A). vRNA-dependent regulators of IFNβ production are members of phenoclusters in which IFNβ levels changed in response to vRNA (211 positive regulators, $P_{1–6}$; 145 negative regulators, $P_{7–12}$). These genes correctly include many well-known regulators of type I IFN, both activators (e.g., VISA, IRF3, RELA, IκBKγ, IκBKε, IκBKβ, and IRF9) and repressors (e.g., PTPN6 and IRF2). Knockdown of some of these genes did not affect PR8 replication ($P_{1,2,7,8}$. e.g., IFNβ in P_1), probably because the NS1 protein already ensures low levels of IFNβ postinfection. Others ($P_{3,4,9,10,}$ e.g., IRF3 and IRF2) had opposing effects on IFN levels and viral replication, including genes ($P_{4,10}$) that were essential for IFNβ-dependent antiviral effects even in NS1-inhibited cells. Genes that were not previously known to affect IFN production included a potential ubiquitin ligase complex (CUL1 and FBXO34), regulators of vesicle trafficking (e.g., CHMP6 and ARL4A), peroxisomal components (PEX14), WNT pathway genes (below), and genes known to be involved in the life cycle of other viruses (e.g., TMF1 binding to the HIV TATA element (Table S5) (Garcia et al., 1992).

Virus-dependent, vRNA-independent regulators of IFNβ production (137 genes, $P_{13–14}$, $P_{17–20}$) affect ΔNS1-induced, but not vRNA-induced, IFN production. These are subdivided into genes that do not affect ($P_{13,14}$), inversely affect ($P_{19,20}$), or concordantly affect PR8 replication ($P_{17,18}$; we cannot rule out the possibility that these genes affect IFN production as a consequence of their effect on replication). These genes include PRKRA, a known regulator of PKR (in P_{20}) and TRAF6 (in P_{13}), known essential regulators of PR8 replication such as NXF1 (P_{17}) and PGD (P_{17}) (Hao et al., 2008; Satterly et al., 2007), and inflammasome-associated components (NOD2 and NLRP9, P_{18}), consistent with recent findings (Sabbah et al., 2009). We also observe candidates such as TTC12 (P_{18}) that associates physically with PB1 (Figure 2B). PKR, a known repressor of viral replication, is also a member of this group (P_{14}) and shows no effect on PR8 replication in our assay. This probably reflects masking of PKR activity by the NS1 protein (Li et al., 2006), suggesting that other regulators of viral replication masked by NS1 are members of this class.

IFN-independent regulators of viral replication (107 genes, P_{15}–P_{16}) are genes that affected PR8 replication, but did not affect IFN production. These include PML, an "H_2" gene and a well-established negative regulator of viral replication (Everett and Chelbi-Alix, 2007), and a previously unappreciated negative

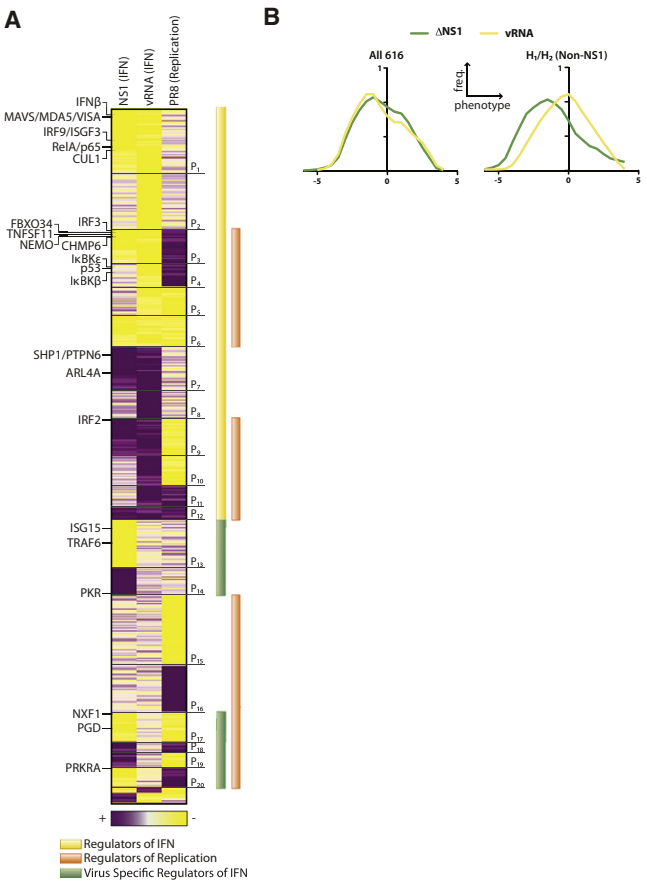

Figure 4. Functional Interrogation and Classification of Candidate Genes Identified through Integrative Analysis of Influenza-Human Interactions

(A) Classification of phenotypes resulting from siRNA-mediated knockdown of 616 genes. The heat map shows phenotype scores corresponding to three functional assays (columns) performed on HBECs after transfection with siRNAs (rows). Gene phenotypes are hierarchically clustered, resulting in 20 major phenoclusters ($P_{1–20}$). NS1 (IFN), assay for production of interferon after infection with ΔNS1 virus; vRNA (IFN), assay for production of interferon after transfection with viral RNA; PR8 (Replication), assay for infectious virion production after infection with PR8 virus. Yellow, positive regulator (lower IFN or virus titer); purple, negative regulator (higher IFN or virus titer). Selected genes (also referred to in the main text) are marked (left).

(B) Distribution of phenotype scores for direct physical interactors and their first neighbors. H_1/H_2 interactors (excluding NS1) show a significantly higher number of positive regulators of interferon production after infection with ΔNS1 (green) compared to vRNA transfection (yellow) (right). There is no such shift in the distribution for all 616 genes shown in the phenocluster heat map (left).

regulator, USHPB1, that interacts physically with PB1 and PB2 (Figure 2B and Table S1 part B). P_{15} includes several candidate positive regulators of replication, including RIOK3, which is induced only by PR8 virus (C_8), and ZMAT4, which interacts directly with M1/PB1/NS1 (Figure 2B).

We next determined the relative contribution of transcriptionally regulated genes to each of the phenoclusters. VSRGs that are induced by both PR8 and ΔNS1 infection (C_7) included 30 genes with effects in our functional assays. This class of genes was enriched in phenotypes ($p < 0.007$) with (mostly positive) effects on IFN production in ΔNS1. The observation that a wild-type virus and a virus lacking NS1 could induce IFN activators suggests that cells may possess RIG-I-independent mechanisms to initiate the antiviral IFN response.

A Subnetwork of RNA-Binding Proteins Affects IFNβ Production during Infection

The functional assays revealed the importance of a number of densely connected areas of the influenza-cellular interaction network (Figure S1). One of these areas was enriched for RNA-binding proteins ($p < 10^{-4}$, Figure S1), including the known regulator PKR, and RBPMS, ILF3, FMR1, DHX9, ZNF346, and HNRPC. ILF3 is phosphorylated by PKR and associates with XBP-1 (both are key mediators of the stress response [Patel et al. 1999]), and ILF3 in turn interacts with DHX9 and HNRPC (Reichman et al., 2003). Since influenza is an RNA virus, this enrichment may reflect direct regulation of the influenza life cycle. Indeed, we found that short hairpin RNA (shRNA)-mediated depletion of four of these genes significantly affected interferon production after ΔNS1 infection (Figure 5A), with two as negative regulators (PKR and ILF3), and two as positive regulators (DHX9 and HNRPC).

WNT Pathway Components Modulate Cellular Responses to Infection

Another highly enriched subnetwork involved components of the WNT signaling pathway. There is a significant number of interactions between influenza proteins and members of the WNT/β-catenin pathway, and deletion of WNT pathway components significantly impacts influenza replication and interferon production (Figure S6). Consistently, recent studies have implicated the WNT pathway in the modulation of immune function (Staal et al., 2008) and in regulating cell survival and proliferation in EBV infected B cells (Hayward et al., 2006). To test the involvement of the WNT pathway in influenza pathogenesis, we measured the effect of WNT3α treatment on interferon production after influenza infection or vRNA transfection. We found that direct treatment of cells with WNT3α increased IFN production in both assays (Figures 5B and 5C). The mechanism of action is yet to be defined.

The Viral Polymerase May Mediate a Non-NS1 Effect on IFNβ Production

The non-NS1 physical interactors and their direct neighbors (non-NS1 H_1/H_2) have a higher number of positive regulators of interferon production in the ΔNS1 assay than in the vRNA transfection assay ($p < 0.001$, Kolmogorov-Smirnov test, Figure 4B, right). This distinction is in marked contrast to the overall similarity in phenotypic effects of all the remaining genes (i.e., 616 non-H_1/H_2 genes) on IFNβ production in both assays (Figure 4B, left). This suggested that non-NS1 viral proteins participate in the manipulation of IFN production in response to viral RNA.

To identify candidate non-NS1 mechanisms that mediate the effect on IFN production, we ranked each of the viral proteins based on their neighborhood enrichment for cellular pathways. The most prominently enriched neighborhoods of non-NS1

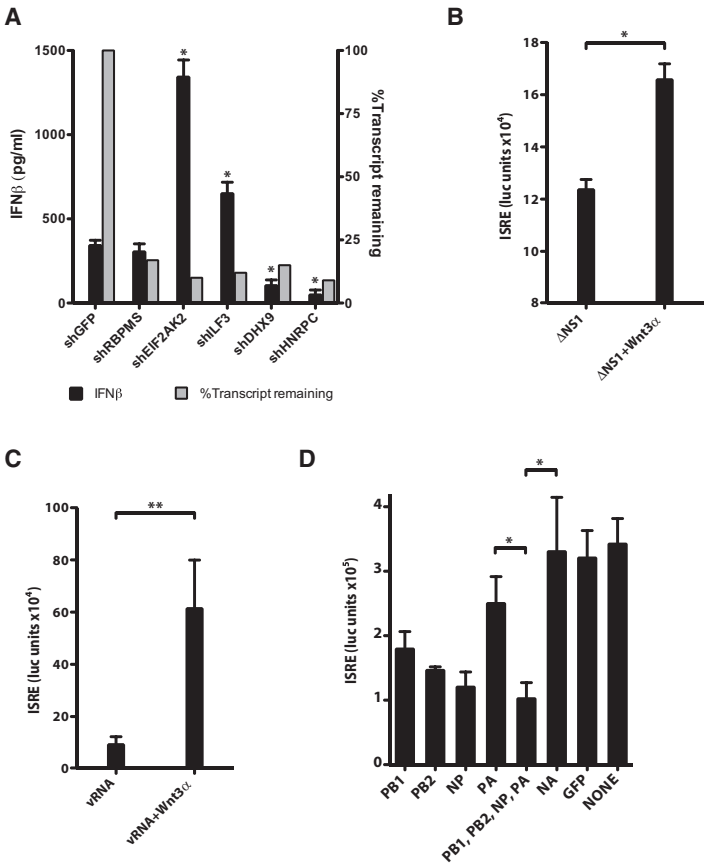

Figure 5. Functional Roles of an RNA-Binding Protein Subnetwork, the WNT Pathway, and the Viral Polymerase

(A) RNA-binding proteins play a role in regulating interferon production in HBECs infected with ΔNS1 virus. HBECs were infected with lentiviral shRNAs to knockdown each of five candidate RNA-binding proteins. Cells were selected in puromycin for 5 days and then stimulated with ΔNS1 virus. Supernatants were collected 24 hr postinfection, and IFNβ protein levels were quantified by ELISA (black bars, left y axis). In the same experiment, the efficacy of knockdown by each shRNA on its target mRNA was quantified (gray bars, right y axis, measured by qPCR relative to GAPDH). (n = 3.)

(B and C) WNT protein potentiates ISRE responses in epithelial cells. 293T-ISRE-luciferase reporter cells were treated with WNT3α for 24 hr and then infected with ΔNS1 virus or transfected with vRNA for 18 hr. Luciferase reporter activity (y axis) was quantified in response to ΔNS1 infection (B) or transfected vRNA (C) (purified from PR8 virions). (n = 6.)

(D) Overexpression of viral polymerase subunits or NP and their effects on ISRE-inducing activity after vRNA transfection. 293T-ISRE-luciferase reporter cells were transfected with an expression plasmid encoding each influenza polymerase subunit or with combinations of plasmids (bottom panel) and then stimulated with transfected vRNA. ISRE responses to transfected vRNA were quantified for each of PB1, PB2, NP, PA, NA, control GFP, and their combinations. Similar results were obtained when cells were infected with ΔNS1 virus (data not shown). Significant effects of overexpression were found only for PB1, PB2, NP, and PB1/PB2/NP/PA versus NA (but only two are marked for clarity). (n = 6.)

Error bars represent the standard deviation of the replicates. *$p < 0.05$ (t test).

proteins were for two of the three viral polymerase subunits (PB1 and PB2) and NP (Table 1, Figure 3D). These neighborhoods are also conserved in the Udorn strain ($p < 10^{-10}$, hypergeometric test), and are enriched for VSRGs (C_6) whose expression is induced only in ΔNS1 infection. We thus hypothesized that the viral polymerase may play a previously unappreciated, NS1-independent, role in modulating interferon production.

To test this hypothesis, we measured the effect of overexpressing viral-polymerase subunits and NP on cellular production of IFN. Indeed, we found that overexpression of PB1, PB2, and NP, individually and in combination, was sufficient to inhibit cellular interferon responses to either vRNA transfection or ΔNS1 infection (Figure 5D). This disruptive effect is more prominent for PB1, PB2, and NP than for PA. This is consistent with the lower enrichment of the PA neighborhoods across immune functions and pathways and with the lower connectivity of PA in the PR8 and Udorn interaction networks (Figure 3D, Table 1). Taken together, our results illustrate the functional relevance of the Y2H interactions and implicate non-NS1 viral proteins modulating host responses.

DISCUSSION

A Physical, Regulatory, and Functional Map of Influenza-Host Interactions

Influenza-host interactions have evolved over countless infections across diverse host species. To capture this complex relationship, we have constructed a first comprehensive map representing the physical and regulatory interactions between influenza virus and its primary human host cell. First, we assembled a physical map of binary associations between human and viral proteins. Second, we defined the regulatory responses of the host using genome-wide mRNA profiling of HBECs exposed to wild-type virus, ΔNS1 virus, viral RNA, or type I IFN. Third, we overlaid these maps within the context of known cellular human networks, expanding them to a neighborhood of the human interaction network and annotated cellular pathways. This led us to identify 1745 candidate genes that may play a role in influenza replication or the host response to infection. To validate the function of these candidate genes, we assessed the loss-of-function effects of each of the candidates in three independent in vivo assays in HBECs and classified each gene within a specific phenocluster. These extensive experimental and computational analyses allowed us to assign to each candidate gene a physical, transcriptional, and phenotypic "fingerprint" that reflects its specialized role in the host-pathogen network (Table S5).

Our results must be interpreted with care, and additional experiments, such as in vivo pulldown assays during infection, will be needed to further validate and refine the network. Furthermore, we conservatively scored our functional assays, and may have masked relevant false negatives. Finally, analyses across other influenza strains may further generalize our findings. Nevertheless, by integrating across three sources of information,

we were able to reveal new roles for viral and host proteins in manipulating the cellular machinery during infection.

Effects of the NS1 Protein May Be Mediated by the p53 and WNT Pathways

We rediscovered many of the known roles and interactions of the well-studied PR8 and Udorn NS1 proteins. For example, these included NS1-dependent dampening (Figure 3A) of the RIG-I-mediated transcriptional response to RNA (Pichlmair et al., 2006) and the direct interaction between NS1 and proteins involved in RIG-I/NFκB, PKR, and mRNA processing functions (Figure 2B).

We also expanded the physical and regulatory scope of NS1 in the context of viral infection. We suggest a regulatory role for NS1 in the induction of 45 RNA/IFN-independent VSRGs ($C_{8,12}$, Figure 3), 24 of which impact viral replication or the host IFN response in our assays (Table S5). We found previously unknown physical associations between NS1 and multiple proteins of the p53 and WNT pathways (Figures 2B and 2C). Components of these pathways affect the host response to virus in our assays (Table S5), and direct treatment with recombinant WNT protein increases cellular production of IFN in response to vRNA and viral infection (Figures 5B and 5C). While further experiments are required to understand the mechanistic basis of these findings, we propose that NS1 protein has an even broader impact on cellular processes than was previously appreciated.

A Potential Role for the Viral Polymerase in Host-Pathogen Interactions

We discovered a large number of proteins and pathways, including the NF-κB, p53, apoptosis, and WNT pathways, that physically associate with the two viral polymerase subunits PB1 and PB2, and with NP of the PR8 and Udorn strain (Figures 2B and 2C) pathways. In addition, these host components are enriched in VSRGs, suggesting that the virus has also evolved to indirectly regulate mRNA levels of genes in these networks. Consistently, overexpression of one or more of the viral polymerase proteins (or NP) inhibits the IFN response to virus or vRNA in epithelial cells. Further experiments, including disruption of individual virus-host protein interactions (e.g., PB2-TRAF2 versus PB2-DVL3) through point mutations, are needed to exclude nonspecific effects and to further establish these mechanisms.

Virus-Specific Regulated Genes Play an Important Role in Host Defense

Transcriptional profiling of cells exposed to viruses or intermediate components of infection led us to discriminate a group of genes (VSRGs, $C_{6–8,11–12}$) that respond only to virus but not to vRNA or IFN treatment. Many of these have not been previously described in this context. VSRGs include major components of the signaling pathways identified in the physical network, as well as regulators of IFN production and viral replication (Figure 3D, Table S5). How VSRGs are regulated and whether they are specific to influenza virus or respond to a broader class of viruses remains to be determined.

Toward an Integrated Model of Host-Influenza Interactions

To build a model of the core networks targeted by the virus (Figure 6), we focused on the four main pathways identified in our analysis as key targets of the virus both physically and transcriptionally: NFκB (including RIGI and PKR), apoptosis, MAPK, and WNT. We incorporated all the H_1 proteins that directly associate with these pathways into the model (see the Experimental Procedures). We annotated each protein in the model with its mode of regulation (physical or transcriptional), the specific viral protein with which it associates, and the functional consequences on IFN and replication upon its knockdown.

We find that the virus targets diverse signaling pathways by affecting multiple components in each pathway through both physical and regulatory interactions. While the same pathway is often targeted by both mechanisms, the direct effect can be mediated through distinct genes. This observation emphasizes the virus' capacity for combinatorial regulation of cellular processes, and the importance of an integrated analysis approach for revealing a more complete picture of the viral-human relationship.

Many unrelated viruses (e.g., HSV, HIV, EBV, and KSHV; Table S4 part B) also target the same proteins or pathways as influenza (Brander and Walker, 2000; Hiscott et al., 2006). For example, HIV targets NFKB1, p53, and β-catenin, and EBV targets TRAF1/2 (Luftig et al., 2004) and SP100. Also consistent with other viruses (König et al., 2008), perturbation of H_1 proteins does not typically result in a phenotypic change. Nevertheless, for influenza, perturbation of a subset of the H_1 proteins (e.g., TARBP2, BANP, STAU1, and PPP2R5C; see Figure 6) does affect IFN production in response to vRNA, suggesting that the virus may inhibit their function by direct binding. In addition, based on the conservation of interactions across PR8 and Udorn, it is likely that some of these extend to other influenza viruses (e.g., the current H5N1, swine H1N1, and other pathogenic strains) and represent candidates for therapeutic targeting.

Our analysis identified the involvement of several pathways whose role in the host response had not been fully appreciated. For example, we found that a group of inflammasome-related sensors are important in modulating IFN production (NLRP14, NOD2, NLRP9, and NLRP10) and virus replication (NOD2). The WNT, p53, ER stress, apoptosis, and PML pathways also impact IFN and replication. Finally, we identified host proteins that were not previously associated with influenza, each of which interacts with multiple viral proteins and is essential for the control of PR8 viral replication (e.g., USHBP1, ZMAT4, and MAGEA11). Such proteins are located at the host-pathogen interface and are likely to mediate essential viral and host activities. Among these are several RNA-binding proteins, whose function we validated in an independent assay (Figure 5A).

With rapid advances in comprehensive measurement and perturbation technologies, we will be able to produce increasingly detailed maps of the physical and regulatory interactions underlying viral-host relationships. Such models could provide a basis for interrogating host circuitry across human individuals to help identify host susceptibility factors and causal genetic polymorphisms. Indeed, there is a significant overlap between

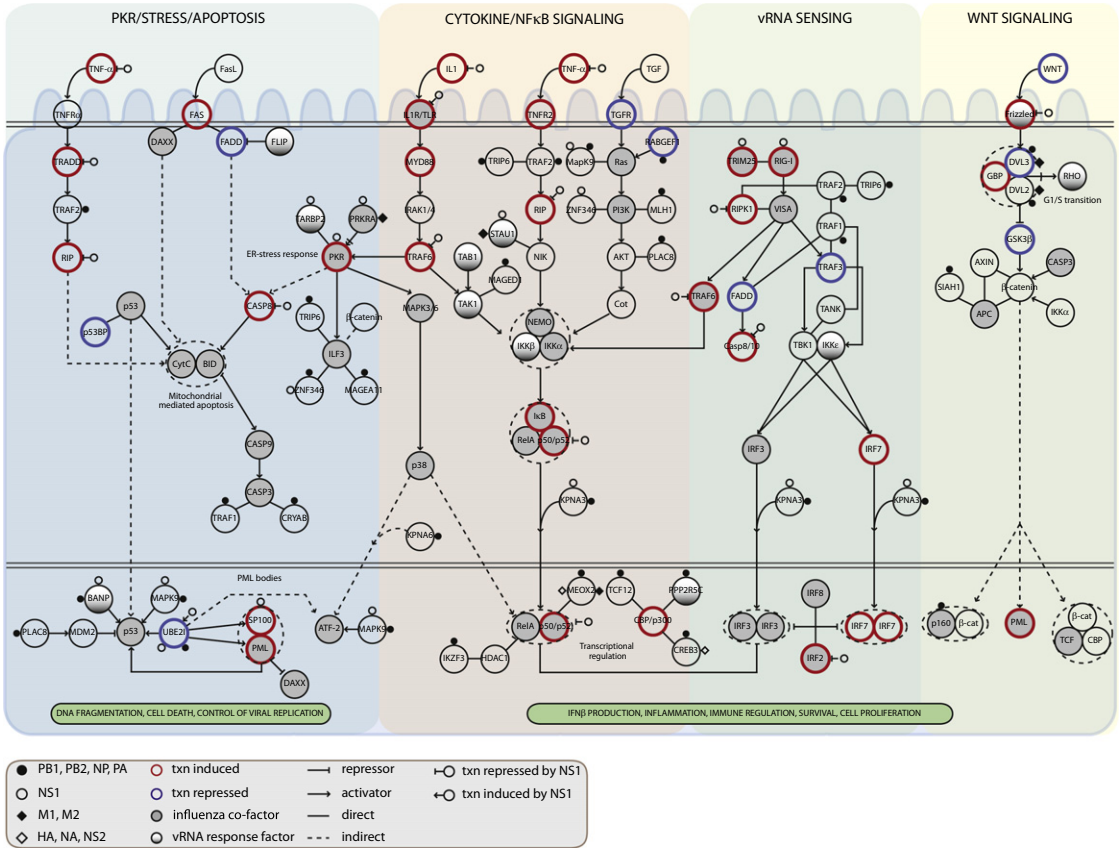

Figure 6. An Integrated Model of the Key Signaling Pathways Modulated by Influenza-Host Interactions

For each host component within computationally selected pathways (see text), we show its mode of regulation and its functional role: (1) Direct physical contact with viral proteins (small circles and diamonds); NS1 interactions with PKR, RIG-I, TRIM25 were added manually based on previous reports; (2) transcriptional regulation in response to influenza infection in HBECs (increase in gene expression, thick red border; decrease, thick blue border); (3) transcriptional regulation by the NS1 protein (open circle with inhibitory edge or activating edge); (4) role in modulation of IFN production or PR8 replication (filled, gray); or role only in the IFN response to vRNA (filled, gradient). Txn, transcriptional. Influenza cofactor indicates significant change in PR8 replication upon siRNA knockdown of that gene. vRNA response factor indicates a gene whose knockdown caused significant change only in the vRNA-induced interferon assay.

the proteins in our model and the genes induced in patients during influenza infection (data not shown). Comprehensive models could also help explain differences in the host response to influenza infection, when the virus is transmitted from one species to another. While some physical and regulatory interactions and their effects on cell function are likely conserved across birds, pigs and humans, others may be host specific and could help account for the differences in virulence across pathogenic strains.

EXPERIMENTAL PROCEDURES

Primary Cell Cultures and Virus Strains

Primary HBECs (Lonza, Basel, Switzerland) derived from normal human bronchial epithelium were maintained in vented T225 tissue culture flasks and grown in bronchial epithelial cell basal medium (Lonza, Supplemental Data). All experiments were performed with low passage (P) cells (P2–P5). Both PR8 and ΔNS1 viral strains were grown in Vero cells (which allow efficient growth of the ΔNS1 virus) in serum-free DMEM with 10% BSA and 1 μg/ml TPCK trypsin. Viral titers were determined by standard MDCK plaque assays.

Yeast Two-Hybrid Assays

Stringent Y2H assays were carried out as described (Venkatesan et al., 2009) with open reading frames (ORFs) from PR8 and Udorn strains as DB-ORFs in MATα Y8930 yeast and against the Human ORFeome v3.1 as AD prey in MATa Y8800. Each primary screen was done twice, and all initial positive pairs from the two primary screens were individually retested three times with fresh stocks of DB-Flu and AD-Human yeast strains. The final data sets contain those interaction pairs that successfully retested at least two times without exhibiting autoactivation of the yeast HIS3 reporter gene (Rual et al., 2005; Venkatesan et al., 2009).

Human Interaction Network

We generated a comprehensive human interaction network by combining information from the interaction databases BioGRID, BIND, and INTACT. To maximize coverage across the network, we included direct binary interactions, cocomplexes, and protein modifications. In total, the network contained 57,206 interactions among 11,624 human proteins. To analyze the first neighbors of H_1 proteins (H_2), we used both curated and noncurated resources. Noncurated neighbors consisted of 1923 human proteins that physically interact with H_1 proteins based on the human interaction network. Curated first neighbors consisted of 653 human proteins that interact directly with H_1 proteins based on the Ingenuity Pathway Analysis (IPA) Interactions Knowledge Base (Ingenuity, Redwood City, CA), when including only direct

relationships among proteins (i.e., excluding transcription regulation, protein-DNA interactions and protein-chemical relations). The statistical analysis of connection degrees around viral host proteins was calculated by permutation testing (n = 10000). All reported p values for network connections were adjusted for multiple testing with a false discovery rate (FDR) correction ($p < 0.05$).

Functional Annotations

All gene lists for 36 functional categories were downloaded from the IPA database. We also tested all 29 relevant categories specified by the GO Slim generic list (Ashburner et al., 2000) and augmented it with an additional seven immune-related Ingenuity categories. All p values for functional enrichments were adjusted for multiple testing with an FDR correction ($p < 0.05$).

Pathway Analyses

We collected 646 cellular pathway gene sets, including the MSigDB (Subramanian et al., 2005) "canonical pathways" collection and viral-response pathway gene sets from IPA. We grouped these into 212 distinct pathway groups (Figure S7) to avoid redundancies. We tested whether the H_1 proteins and their curated first neighbors (H_2), and each expression cluster was overrepresented in the pathway gene set (a hypergeometric enrichment test; the same result was obtained when using the noncurated H2 set, Figure S8). All p values were adjusted for multiple testing with an FDR correction ($p < 0.05$).

mRNA Expression Profiling

HBECs were stimulated with a 15 min pulse of 1000 U/ml IFNβ (PBL, Piscataway, NJ), 100 ng/ml vRNA (purified directly from PR8 virus) with LTX transfection reagent (Invitrogen, Carlsbad, CA), wild-type H1N1 influenza (A/PR/8/34), or ΔNS1 virus (PR8 with a deleted NS1 gene, a gift from Dr. Garcia-Sastre). Viruses were used at a multiplicity of infection (moi) of 5. Control samples were incubated with media or LTX under the same conditions. Cells were washed, supplemented with warm media, and harvested at 11 time points (0, 0.25, 0.5, 1, 1.5, 2, 4, 6, 8, 12, and 18 hr posttreatment).

Array Hybridizations and Preprocessing

All array hybridizations and preprocessing were done with Affymetrix HT Human Genome U133 Arrays (see the Supplemental Data). We defined the fold change of each gene in a stimulated sample as the average intensity of its probe set in two biological replicates, normalized by its *expected* intensity at the same time point without treatment. To calculate the expected intensities, genes were clustered based only on their intensities in the mock treatment (PCluster [Segal et al., 2003], n = 30). For each time point, all genes within a cluster were compared to the same expected intensities (i.e. the average intensities of the particular mock time point across the entire cluster). To identify genes whose expression is affected by stimulation, we selected genes with $\geq$1.6-fold change in two consecutive time points (or $\geq$2-fold for each of the single time points, 12 hr or 18 hr) (Table S6). At this threshold, we expect a 10% error rate, estimated by the number of genes that cross the cutoff in mock LTX (false positives) versus $vRNA^{+}$LTX transfection (true positives; data not shown).

Clustering of Expression Data

We clustered the time-series gene expression data by a modification of the PCluster algorithm. We first applied PCluster (k = 30) as previously described (Segal et al., 2003) and then iteratively improved the partition. There are two steps at each iteration: (1) splitting and (2) merging of clusters. The splitting step learns the best partition of each cluster into two clusters, through a search over every pair of consecutive time points. The query that best partitions the gene expression at two consecutive time points into two distinct distributions is chosen until no significant split exists (t test p value cutoff of 10^{-23}). In the merging step, we merge pairs of clusters that are not significantly distinct in any two consecutive time points (same t test cutoff). This fits our sparse temporal information, when many genes are only regulated in a few consecutive time points (e.g., $C_{6,8}$). The 35 resulting clusters were grouped manually into 12 categories called "expression clusters" (Figures 3A and 3B, C_1–C_{12}). Expression cluster 1 (C_1) includes those clusters that overlap but do not clearly fall into any of these categories.

siRNA Transfection and Stimulation of Primary HBECs

HBECs (3.5×10^3, filtered through a 0.4 μm filter) were seeded in wells of triplicate 96-well plates. Twenty-four hours later, 25 nM (final concentration) of siRNA duplexes (SMARTpools, Dharmacon) were transfected (HiPerFect, QIAGEN) and incubated at 37°C for 3 hr, followed by a media change. Cells were incubated for 3 days with one media change at 24 hr posttransfection. After knockdown, we used AlamarBlue (Invitrogen, Carlsbad, CA) to determine live cell numbers in all wells (in some replicate plates). Cells were then washed twice with complete media. To assess the effects of siRNAs on influenza virus replication, cells were inoculated with PR8 virus at a moi of 1. At 48 hr postinfection, HBEC supernatants were harvested and frozen with 5 μg/ml TPCK trypsin. To assess effects on IFN production in response to vRNA and ΔNS1, cells were transfected with 100 ng/ml vRNA or infected with ΔNS1virus at a moi 5. At 24 hr posttransfection or infection, HBEC supernatants were harvested for IFN assays.

Virus Titering of HBEC Supernatant

293T cells (2×10^6, filtered through a 0.4 μm filter) were seeded in 10 cm dishes and transfected with a vRNA luciferase reporter plasmid based on prior design (Lutz et al., 2005) with Transit-LT1. Cells were trypsinized at 24 hr posttransfection and 10^4 transfected reporter cells were reseeded in white Costar plates. Supernatants (frozen with trypsin) from PR8-infected HBECs were added to reporter cells and incubated for 24 hr. Reporter activity was measured with firefly luciferase substrate (Steady-Glo, Promega, Madison, WI). Luminescence in 96-well plates was quantified with the Envision Multilabel reader (Perkin Elmer, Waltham, MA) fitted with an automated plate stacker.

Determining Interferon Production from HBEC Supernatants

Cells were infected with a lentivirus containing ISRE-luciferase (Cignal Lenti ISRE Reporter, SA Biosystems, Frederick, MD). After selection with puromycin, stably infected cells were cloned by limiting dilution and tested for responsiveness to human IFNβ (PBL, Piscataway, NJ). A clone with high signal to background ratio was selected and found to be sensitive to low levels of IFNβ (<1 U/ml) with a >100× dynamic range. Fro measurement of IFNβ in supernatants from experimental assays, ISRE-Luc reporter cells were seeded in flat bottom white Costar plates at 2×10^4/well. Twenty-four hours later, supernatants were added and assayed for ISRE-Luc-inducing activity with firefly luciferase substrate.

Scoring of Functional Assays and Identification of Phenoclusters

For each assay, luminescence values were quantified with the Envision reader for ISRE-luc and vRNA-luc reporters. These values were normalized with robust Z score normalization (RNAeyes program, A. Derr, Broad Institute) and averaged across three replicates. Robust Z scores were further normalized to cell number per well by calculating the distance of each robust Z score from the running average of robust Z scores versus AlamarBlue values. These cell number-normalized Z scores, referred to as phenotype scores, reduce the impact of cell number variation on assay measurements and allow comparisons across wells and plates. Genes with a phenotype score equivalent to a 2-fold or more change in IFN or replication (compared to the median score for the relevant assay; see the Supplemental Data) in each assay were analyzed further and clustered into 20 "phenoclusters" with single-linkage hierarchical clustering with the Cluster software (Eisen et al., 1998). Statistical enrichments of phenotype scores in expression clusters or pathway gene sets were evaluated by permutation tests (n = 10,000).

ACCESSION NUMBERS

The expression data reported in this publication have been deposited in NCBI's Gene Expression Omnibus and are accessible through GEO Series accession number GSE19392 (http://www.ncbi.nlm.nih.gov/geo/query/acc.cgi?acc=GSE19392).

SUPPLEMENTAL DATA

Supplemental Data include Supplemental Experimental Procedures, eight figures, and six tables and can be found with this article online at http://www.cell.com/supplemental/S0092-8674(09)01565-7.

ACKNOWLEDGMENTS

We thank D. Lieber and K. Maciag for discussions and help with data analysis. We thank C. Shamu and S. Chiang at ICCB (HMS) for the siRNA library and expert advice, S. Gupta and the Broad's Genetic Analysis Platform for microarray processing, H. Le, A. Derr, B. Wong, and the staff at the Broad RNAi Platform for assistance with RNAi studies and analysis, L. Wu for the vRNA reporter plasmid, R. Cadagan and A. Garcia-Sastre for ΔNS1 virus, E. Fodor for PR8 plasmids, R. Lamb for Udorn plasmids, and S. Hart for assistance with artwork. This work was supported by National Institutes of Health (NIH) grant U01 AI074575 (N.H., D.R., and D.H.); U54 AI057159 and the NIH New Innovator Award (N.H.); Ford Foundation Predoctoral Fellowship (M.G.); EMBO Postdoctoral Fellowship (I.G.V.); The Ellison Foundation and NIH grants R01 HG001715 and P50 HG004233 (D.H.); and the Howard Hughes Medical Institute, a Career Award at the Scientific Interface from the Burroughs Wellcome Fund, the NIH Pioneer Award, and the Sloan Foundation (A.R.).

Received: December 2, 2009
Revised: December 9, 2009
Accepted: December 9, 2009
Published online: December 17, 2009

REFERENCES

Ashburner, M., Ball, C.A., Blake, J.A., Botstein, D., Butler, H., Cherry, J.M., Davis, A.P., Dolinski, K., Dwight, S.S., Eppig, J.T., et al., The Gene Ontology Consortium. (2000). Gene ontology: tool for the unification of biology. Nat. Genet. *25*, 25–29.

Bailer, S.M., and Haas, J. (2009). Connecting viral with cellular interactomes. Curr. Opin. Microbiol. *12*, 453–459.

Brander, C., and Walker, B.D. (2000). Modulation of host immune responses by clinically relevant human DNA and RNA viruses. Curr. Opin. Microbiol. *3*, 379–386.

Brass, A.L., Dykxhoorn, D.M., Benita, Y., Yan, N., Engelman, A., Xavier, R.J., Lieberman, J., and Elledge, S.J. (2008). Identification of host proteins required for HIV infection through a functional genomic screen. Science *319*, 921–926.

Bushman, F.D., Malani, N., Fernandes, J., D'Orso, I., Cagney, G., Diamond, T.L., Zhou, H., Hazuda, D.J., Espeseth, A.S., König, R., et al. (2009). Host cell factors in HIV replication: meta-analysis of genome-wide studies. PLoS Pathog. *5*, e1000437.

Eisen, M.B., Spellman, P.T., Brown, P.O., and Botstein, D. (1998). Cluster analysis and display of genome-wide expression patterns. Proc. Natl. Acad. Sci. USA *95*, 14863–14868.

Everett, R.D., and Chelbi-Alix, M.K. (2007). PML and PML nuclear bodies: implications in antiviral defence. Biochimie *89*, 819–830.

Gack, M.U., Albrecht, R.A., Urano, T., Inn, K.S., Huang, I.C., Carnero, E., Farzan, M., Inoue, S., Jung, J.U., and García-Sastre, A. (2009). Influenza A virus NS1 targets the ubiquitin ligase TRIM25 to evade recognition by the host viral RNA sensor RIG-I. Cell Host Microbe *5*, 439–449.

Garcia, J.A., Ou, S.H., Wu, F., Lusis, A.J., Sparkes, R.S., and Gaynor, R.B. (1992). Cloning and chromosomal mapping of a human immunodeficiency virus 1 "TATA" element modulatory factor. Proc. Natl. Acad. Sci. USA *89*, 9372–9376.

Hale, B.G., Randall, R.E., Ortín, J., and Jackson, D. (2008). The multifunctional NS1 protein of influenza A viruses. J. Gen. Virol. *89*, 2359–2376.

Hao, L., Sakurai, A., Watanabe, T., Sorensen, E., Nidom, C.A., Newton, M.A., Ahlquist, P., and Kawaoka, Y. (2008). Drosophila RNAi screen identifies host genes important for influenza virus replication. Nature *454*, 890–893.

Hayward, S.D., Liu, J., and Fujimuro, M. (2006). Notch and Wnt signaling: mimicry and manipulation by gamma herpesviruses. Sci. STKE *2006*, re4.

Hiscott, J., Nguyen, T.L., Arguello, M., Nakhaei, P., and Paz, S. (2006). Manipulation of the nuclear factor-kappaB pathway and the innate immune response by viruses. Oncogene *25*, 6844–6867.

König, R., Zhou, Y., Elleder, D., Diamond, T.L., Bonamy, G.M., Irelan, J.T., Chiang, C.Y., Tu, B.P., De Jesus, P.D., Lilley, C.E., et al. (2008). Global analysis of host-pathogen interactions that regulate early-stage HIV-1 replication. Cell *135*, 49–60.

Krishnan, M.N., Ng, A., Sukumaran, B., Gilfoy, F.D., Uchil, P.D., Sultana, H., Brass, A.L., Adametz, R., Tsui, M., Qian, F., et al. (2008). RNA interference screen for human genes associated with West Nile virus infection. Nature *455*, 242–245.

Krug, R.M., Yuan, W., Noah, D.L., and Latham, A.G. (2003). Intracellular warfare between human influenza viruses and human cells: the roles of the viral NS1 protein. Virology *309*, 181–189.

Lamesch, P., Li, N., Milstein, S., Fan, C., Hao, T., Szabo, G., Hu, Z., Venkatesan, K., Bethel, G., Martin, P., et al. (2007). hORFeome v3.1: a resource of human open reading frames representing over 10,000 human genes. Genomics *89*, 307–315.

Li, S., Min, J.Y., Krug, R.M., and Sen, G.C. (2006). Binding of the influenza A virus NS1 protein to PKR mediates the inhibition of its activation by either PACT or double-stranded RNA. Virology *349*, 13–21.

Li, Q., Brass, A.L., Ng, A., Hu, Z., Xavier, R.J., Liang, T.J., and Elledge, S.J. (2009). A genome-wide genetic screen for host factors required for hepatitis C virus propagation. Proc. Natl. Acad. Sci. USA *106*, 16410–16415.

Luftig, M., Yasui, T., Soni, V., Kang, M.S., Jacobson, N., Cahir-McFarland, E., Seed, B., and Kieff, E. (2004). Epstein-Barr virus latent infection membrane protein 1 TRAF-binding site induces NIK/IKK alpha-dependent noncanonical NF-kappaB activation. Proc. Natl. Acad. Sci. USA *101*, 141–146.

Lutz, A., Dyall, J., Olivo, P.D., and Pekosz, A. (2005). Virus-inducible reporter genes as a tool for detecting and quantifying influenza A virus replication. J. Virol. Methods *126*, 13–20.

Patel, R.C., Vestal, D.J., Xu, Z., Bandyopadhyay, S., Guo, W., Erme, S.M., Williams, B.R., and Sen, G.C. (1999). DRBP76, a double-stranded RNA-binding nuclear protein, is phosphorylated by the interferon-induced protein kinase, PKR. J. Biol. Chem. *274*, 20432–20437.

Pichlmair, A., Schulz, O., Tan, C.P., Näslund, T.I., Liljeström, P., Weber, F., and Reis e Sousa, C. (2006). RIG-I-mediated antiviral responses to single-stranded RNA bearing 5′-phosphates. Science *314*, 997–1001.

Reichman, T.W., Parrott, A.M., Fierro-Monti, I., Caron, D.J., Kao, P.N., Lee, C.G., Li, H., and Mathews, M.B. (2003). Selective regulation of gene expression by nuclear factor 110, a member of the NF90 family of double-stranded RNA-binding proteins. J. Mol. Biol. *332*, 85–98.

Rual, J.F., Venkatesan, K., Hao, T., Hirozane-Kishikawa, T., Dricot, A., Li, N., Berriz, G.F., Gibbons, F.D., Dreze, M., Ayivi-Guedehoussou, N., et al. (2005). Towards a proteome-scale map of the human protein-protein interaction network. Nature *437*, 1173–1178.

Sabbah, A., Chang, T.H., Harnack, R., Frohlich, V., Tominaga, K., Dube, P.H., Xiang, Y., and Bose, S. (2009). Activation of innate immune antiviral responses by Nod2. Nat. Immunol. *10*, 1073–1080.

Satterly, N., Tsai, P.L., van Deursen, J., Nussenzveig, D.R., Wang, Y., Faria, P.A., Levay, A., Levy, D.E., and Fontoura, B.M. (2007). Influenza virus targets the mRNA export machinery and the nuclear pore complex. Proc. Natl. Acad. Sci. USA *104*, 1853–1858.

Segal, E., Shapira, M., Regev, A., Pe'er, D., Botstein, D., Koller, D., and Friedman, N. (2003). Module networks: identifying regulatory modules and their condition-specific regulators from gene expression data. Nat. Genet. *34*, 166–176.

Staal, F.J., Luis, T.C., and Tiemessen, M.M. (2008). WNT signalling in the immune system: WNT is spreading its wings. Nat. Rev. Immunol. *8*, 581–593.

Subramanian, A., Tamayo, P., Mootha, V.K., Mukherjee, S., Ebert, B.L., Gillette, M.A., Paulovich, A., Pomeroy, S.L., Golub, T.R., Lander, E.S., and

Mesirov, J.P. (2005). Gene set enrichment analysis: a knowledge-based approach for interpreting genome-wide expression profiles. Proc. Natl. Acad. Sci. USA *102*, 15545–15550.

Takeuchi, O., and Akira, S. (2009). Innate immunity to virus infection. Immunol. Rev. *227*, 75–86.

Turpin, E., Luke, K., Jones, J., Tumpey, T., Konan, K., and Schultz-Cherry, S. (2005). Influenza virus infection increases p53 activity: role of p53 in cell death and viral replication. J. Virol. *79*, 8802–8811.

Venkatesan, K., Rual, J.F., Vazquez, A., Stelzl, U., Lemmens, I., Hirozane-Kishikawa, T., Hao, T., Zenkner, M., Xin, X., Goh, K.I., et al. (2009). An empirical framework for binary interactome mapping. Nat. Methods *6*, 83–90.

Wressnigg, N., Shurygina, A.P., Wolff, T., Redlberger-Fritz, M., Popow-Kraupp, T., Muster, T., Egorov, A., and Kittel, C. (2009). Influenza B mutant viruses with truncated NS1 proteins grow efficiently in Vero cells and are immunogenic in mice. J. Gen. Virol. *90*, 366–374.